Title
Multidimensional Correlations in Asymmetric Catalysis through Parameterization of Uncatalyzed Transition States

Journal
Angewandte Chemie International Edition, 56(45)

ISSN
1433-7851

Authors
Orlandi, Manuel
Toste, F Dean
Sigman, Matthew S

Publication Date
2017-11-06

DOI
10.1002/anie.201707644

Peer reviewed

Asymmetric Catalysis

International Edition: DOI: 10.1002/anie.201707644
German Edition: DOI: 10.1002/ange.201707644

Multidimensional Correlations in Asymmetric Catalysis through Parameterization of Uncatalyzed Transition States

*Manuel Orlandi, F. Dean Toste, and Matthew S. Sigman**

Abstract: *The study of the oxidative amination of tetrahydroisoquinolines under chiral-anion phase-transfer (CAPT) catalysis by multidimensional correlation analysis (MCA) is revisited. The parameterization of the transition states (TSs) for the uncatalyzed reaction, the introduction of conformational descriptors, and the use of computed interaction energies and distances as parameters allowed access to a considerably simplified mathematical correlation of substrate and catalyst structure to enantioselectivity. The equation obtained is suggestive of key interactions occurring at the TS. Specifically, the CAPT catalyst is proposed to coordinate the intermediate iminium cation by P=O···H–O hydrogen-bonding and N···H–C electrostatic interactions. The conformational freedom of the benzyl substituent of the substrate was also found to be important in providing an efficient mode of molecular recognition.*

Recently, multidimensional correlation analysis (MCA) has emerged as a mechanistic tool for transition-state (TS) interrogation in asymmetric catalysis.[1] By this technique, a polynomial equation that correlates the reaction outcome with the chemical descriptors of a catalyst and/or substrate set can be derived. The resultant mathematical model can be used to extrapolate better catalysts through virtual screening, thus improving the reaction performance.[2] Additionally, analysis of the parameters included in the equation provides information about the reaction mechanism.[2b,3] Historically, limited parameters, including Hammett σ,[4] Tolman cone angle,[5] and Charton[6] and Taft parameters,[7] were available to probe such mechanistic considerations. However, modern physical organic descriptors reported more recently[8] have ultimately led to the rationalization of reactions of enhanced complexity.[3b,9] Even with these advances and the ability to perform multivariate analysis of intricate processes for predictive purposes, in some cases the sophistication of the reaction does not lend itself to straightforward analysis. As an example, we reported the correlation of both substrate and catalyst descriptors to enantioselectivity in the oxidative amination of tetrahydroisoquinolines under chiral-anion phase-transfer (CAPT)[10] catalysis (Figure 1 A). In that study, a data-intensive approach was used to obtain a complex mathematical model that allowed extrapolation of the improved catalyst **1a** (Figure 1 B, C). In this model, several IR[9b] intensity and frequency parameters for the triazole moiety suggested the presence of noncovalent interactions (NCIs) between the ring and the substrate in the TS (Figure 1 C), yet it was not possible to build a descriptive picture of the interactions at the heart of the asymmetric catalysis. Thus, we came up with a unique strategy to develop a parameter set suited to this complex problem. Specifically, we envisioned applying our recently introduced computed interaction energies $E\pi$ and distances $D\pi$,[3d] which could provide specific insight into the influential NCIs. Of greater importance, we hypothesized that the readily computed

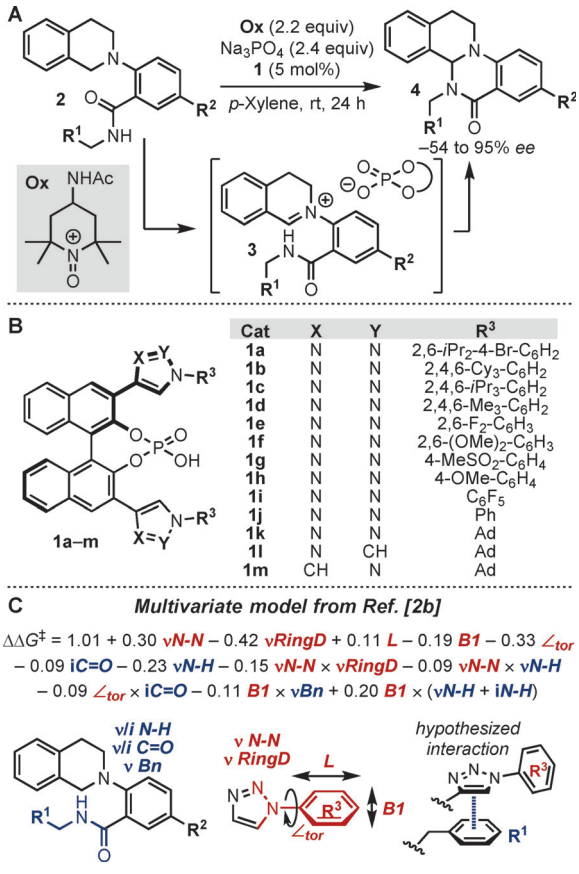

Figure 1. A) Case study: Oxidative amination of tetrahydroisoquinolines. B) CAPT catalysts considered in the present study. C) Multivariate model previously reported and interaction hypothesized between the substrate benzyl (Bn) group and the catalyst triazole ring. Ad = adamantyl, Cy = cyclohexyl.

[*] Dr. M. Orlandi, Prof. M. S. Sigman
Department of Chemistry, University of Utah
315 South 1400 East, Salt Lake City (USA)
E-mail: sigman@chem.utah.edu
Prof. F. D. Toste
Department of Chemistry, University of California
Berkeley, CA 94720 (USA)

Supporting information and the ORCID identification number(s) for the author(s) of this article can be found under: https://doi.org/10.1002/anie.201707644.

transition state of the corresponding uncatalyzed cyclization would represent an optimal platform for parameter acquisition owing to its resemblance to the TS of the catalyzed reaction. We posited that this effort would deepen our mechanistic understanding regarding the stereodefining step and the specific molecular-recognition events required for high enantioselectivity.[2b,11] Herein, we describe the application of this approach to significantly simplify the equation describing enantioselectivity and provide a detailed overview of how asymmetric catalysis is effectively achieved.

Owing to the influence that the triazole moieties of the catalyst and the benzyl group of the substrate have on the reaction stereochemical outcome,[2b] the generic interaction in Figure 1C was previously hypothesized. However, other portions of cation **3** may be recognition elements for the catalyst. Hence, interaction energies and distances[3d] were computed at the B97D/def2TZVP level of theory[12] by using three different probes: benzene **PhH** (E/D_{PhH}), iminium cation **ImC** (E/D_{ImC}), and anilinium cation **AnC** (E/D_{AnC}, Figure 2A). These probes describe the possible interaction of one of the triazole rings with three different moieties of intermediate iminium cation **3** (Figure 2A). Specifically, E/D_{PhH}, E/D_{ImC}, and E/D_{AnC}, respectively, account for the possible interactions with the neutral benzyl group, with the alkyl portion next to the charged N atom, and with the two electron-poor aryl groups. Other parameters for catalysts **1a–m** were also acquired according to a DFT molecular model that we recently introduced for chiral phosphate catalysts (Figure 2C).[3d,10i] IR frequencies and intensities (ν/i), the dihedral angle α, and Sterimol parameters (*B1*, *B5*,and *L*) for this molecular model were calculated at the M06-2X/def2TZVP level of theory.[13]

The dependence of the reaction enantioselectivity on the CAPT catalyst was investigated by correlation of the selectivities (expressed as $\Delta\Delta G^{\ddagger}$ in kcal mol^{-1}) measured for the cyclization of substrate **2a** (Figure 2B). Among all the parameters collected, **sen(α)** (sine of the dihedral angle α in the catalyst, Figure 2C) was the only single parameter that provided a qualitative trend ($R^2 = 0.66$; see the Supporting Information), thus suggesting the importance of geometric and/or steric requirements for high enantioselectivity to be attained. When a multidimensional correlation was determined, the mathematical model in Figure 2C was obtained ($R^2 = 0.87$, L1O = 0.74, L1O = leave-one-out cross-validation). This equation is composed of three terms: **sen(α)**, which accounts for geometrical/steric requirements; ν_{POsy}, which describes the coordination ability (or Lewis basicity) of the phosphate; and the cross-term $E_{ImC}{\cdot}D_{ImC}$, which suggests the presence of a NCI between the triazole ring and the substrate alkyl portion.

Hence, based on the inclusion of these parameters in the multivariate model (Figure 2C), we hypothesized that the catalyst coordinates intermediate **3** through a dual binding mode. Specifically, the phosphate and the triazole ring could engage the amide group and the electron-poor alkyl chain by H-bonding and electrostatic interactions (ν_{POsy} and $E_{ImC}{\cdot}D_{ImC}$). The presence of bulky groups in a specific region of space (**sen(α)**) would then ensure discrimination of one of the enantiotopic faces in the TS. The computational

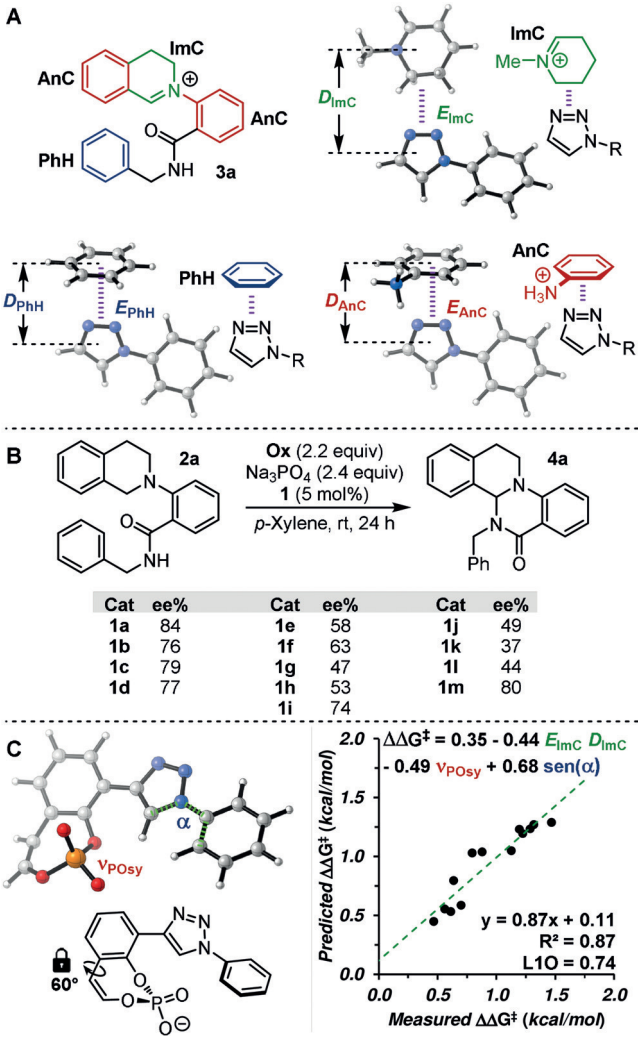

Figure 2. A) Interaction energies and distances calculated in the present study (E/D_{PhH}, E/D_{ImC}, and E/D_{AnC}). B) Selectivities observed in the oxidative cyclization of substrate **2a** with CAPT catalysts **1a–m**. C) Parameters calculated for catalysts **1a–m** and multivariate model obtained.

study of the uncatalyzed reaction provided additional evidence for the hypothesized coordination mode. Transition states **TS-A** and **TS-B** were calculated at the M06-2X/def2TZVP level of theory. They differ in the tautomeric form in which the amide group acts as a nucleophile. In **TS-A**, the amide is in the iminol form and presents a free OH group available for coordination. In **TS-B**, the amide reacts in its most stable tautomeric form, yet shows distortion of the functional group out of planarity (Figure 3A). Thus, **TS-A** is favored by 5.9 kcal mol^{-1}, which suggests that intermediate **3** most likely reacts in its iminol form (Figure 3A).

Evaluation of the electron-density map for **TS-A** highlights the OH proton and the alkyl chain next to the iminium cation as the most electron-poor regions of the structure (Figure 3B). Thus, for these regions to participate in NCIs, it is likely that they will be matched with electron-rich regions of the catalyst. Calculation of the optimized geometry and electron-density map for catalyst **1b** emphasized two impor-

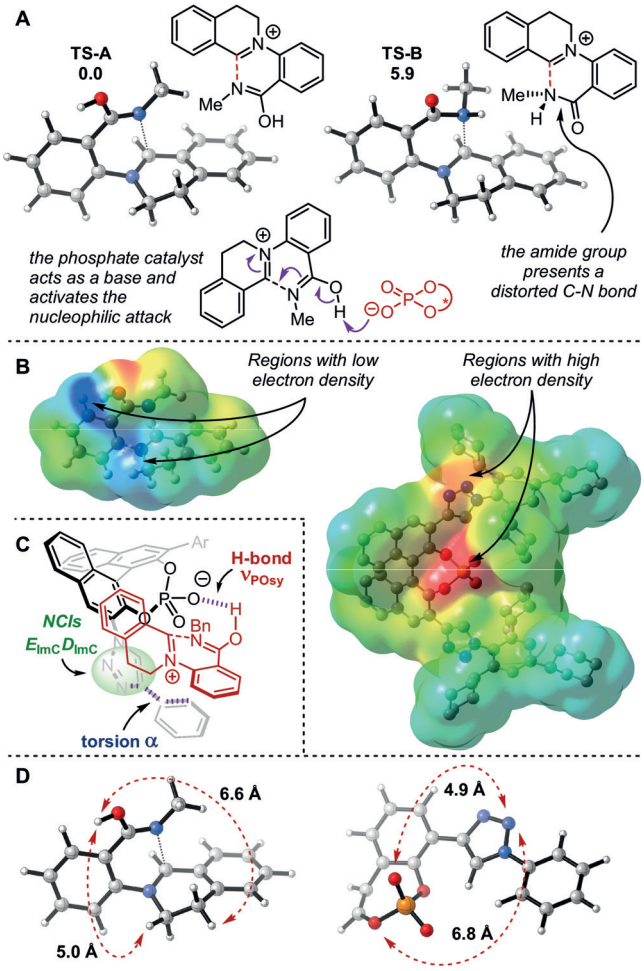

Figure 3. A) Relative energy of tautomeric **TS-A** and **TS-B**. B) Electron-density maps for **TS-A** and **1b**. C) Hypothesized TS for the reaction. D) Distance between electron-poor regions in **TS-A** and electron-rich regions in catalyst **1b**.

tant points: i) the chiral pocket of the catalyst is not accessible owing to steric hindrance, and ii) the most electron rich regions of the catalyst are the phosphate and the triazole groups (Figure 3B). Hence, on the basis of this simple computational analysis and the equation in Figure 2C, we posited the presence of two main interactions that govern the coordination of the reactive intermediate by the catalyst in the transition state. The P=O···H–O hydrogen bond provides coordination and activation of the nucleophilic amide, as the catalyst acts as a Brønsted base (Figure 3A), and the electrostatic interaction between the triazole and the alkyl portion ensure optimal orientation for high stereoselectivity (Figure 3C).[14] Indeed, when such a dual coordination mode is not allowed owing to the substitution of the triazole with a pyrazole or imidazole ring, the selectivity decreases (compare **1m** and **1l**, **1k**, Figure 2B). In other words, the catalyst interacts with intermediate **3** through bidentate binding. Consistent with this hypothesis, the distance between the two electron-poor regions in the substrate and the two electron-rich regions in the catalyst are relatively matched (5.0–6.6 and 4.9–6.8 Å, Figure 3D).

After assessing the role of the catalyst in this transformation, we turned our attention to the dependence of the product *ee* value on the substrate. Although the reaction was found to proceed mainly under catalyst control, the perturbation of the benzyl group of the substrate (especially in the 2,6-positions) resulted in a $\Delta\Delta G^{\ddagger}$ variation of up to 1.5 kcal mol^{-1}. Since phosphate **1** presumably coordinates iminium cation **3** through NCIs, the reagent geometry in the TS of the catalyzed and the uncatalyzed reaction is similar, and the stereoselectivity is due to enhanced structural matching of the catalyst with one of the two enantiomers of such TSs. Thus, the TS of the uncatalyzed reaction represents an optimal structure for substrate parameterization. Additionally, it has fewer conformers than the relative reagent structure, as the presence of the forming C–N bond reduces the molecular degrees of freedom. Hence, descriptors for substrates **2a–k** (Figure 4A) were calculated from the uncatalyzed TSs at the M06-2X/def2TZVP level of theory. The computed parameters include IR frequencies and intensities (**ν**/***i***, including the imaginary frequency associated with C–N bond formation), Sterimol parameters (***B1***, ***B5***, and ***L***), and NBO charges.

As molecular recognition depends on the substrate geometry, the selectivity is due to the ability of the catalyst

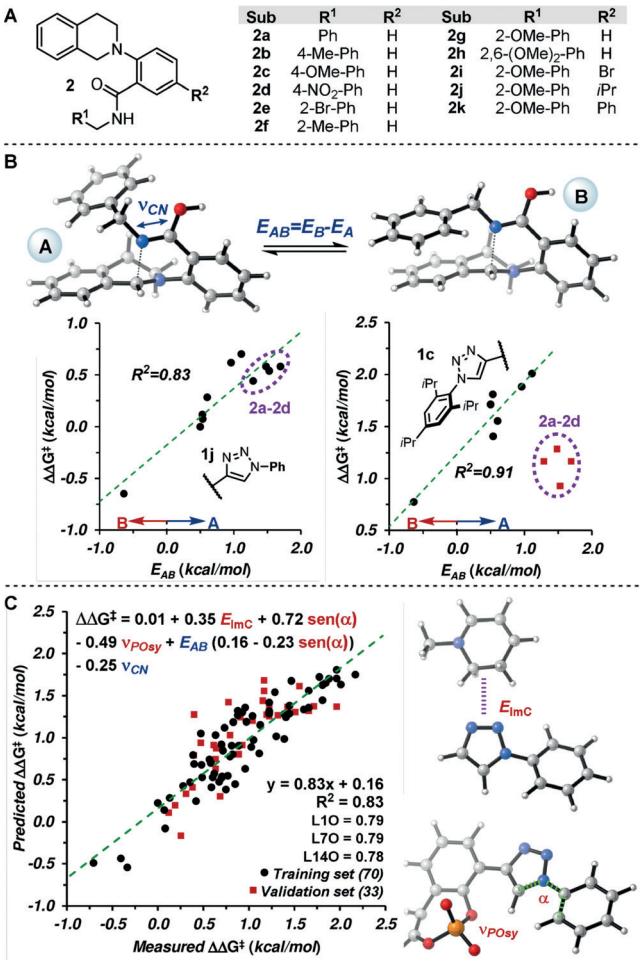

Figure 4. A) Substrates **2a–k** included in the present study. B) Conformational freedom of substrate **2a**. C) Full multidimensional model obtained from 103 data points, and parameters included in the model.

to match with one of the two enantiomeric forms of the uncatalyzed TS in a specific conformation. Hence, we reasoned that the conformational freedom of the benzyl group could be important for optimal interactions. Thus, the energy difference $\boldsymbol{E}_{\mathbf{AB}}$ between the two main conformers of the computed uncatalyzed TSs (structures **A** and **B**, Figure 4B) was included as a parameter in addition to IR, Sterimol, and NBO charge descriptors. Interestingly, $\boldsymbol{E}_{\mathbf{AB}}$ provided good single-parameter correlations (Figure 4B) with $\Delta\Delta G^{\ddagger}$ for both catalyst **1b** and **1j**, which present different steric environments. However, whereas such correlation for substrates **2e–k** shows the same trend for different catalysts, substrates **2a–d** are outliers for bulky catalysts **1a–c** (Figure 4B).

Having determined the new set of parameters, we identified a multidimensional model from the combination of catalysts **1a–j** and substrates **2a–k** (see the Supporting Information for the full list). This model includes 103 data points (70 for the training set and 33 for the external validation set) and includes only six terms (Figure 4C). A 13-term equation (Figure 1C) was previously required for the description of this complex reaction system.[2b] The parameters included in the equation are as follows: $\mathbf{sen}(\boldsymbol{\alpha})$, $\boldsymbol{\nu}_{\mathbf{POS_y}}$, and $\boldsymbol{E}_{\mathbf{ImC}}$ for the catalyst, which also appeared in the equation in Figure 2B; $\boldsymbol{E}_{\mathbf{AB}}$ and $\boldsymbol{E}_{\mathbf{AB}}\cdot\mathbf{sen}(\boldsymbol{\alpha})$, which account for the conformational freedom of the substrate ($\boldsymbol{E}_{\mathbf{AB}}$) and for the ability of the catalyst to recognize the substrate conformation on the basis of its geometry ($\boldsymbol{E}_{\mathbf{AB}}\cdot\mathbf{sen}(\boldsymbol{\alpha})$); and $\boldsymbol{\nu}_{\mathbf{CN}}$ (stretching frequency of the C=N bond in the uncatalyzed TS), which may describe the substrate nucleophilicity. The multivariate model presents $R^2 = 0.83$ and both external and cross-validations (LKO, leave-K-out tests) assess its robustness. Hence, the parameters involved in the full model suggest the coordination mode depicted in Figure 3C. Since the reaction proceeds mainly under catalyst control,[2b] parameters for the catalysts have larger coefficients. Specifically, the ability of the catalyst to coordinate iminium **3** through H-bonding ($\boldsymbol{\nu}_{\mathbf{POS_y}}$) and N···H–C electrostatic interactions ($\boldsymbol{E}_{\mathbf{ImC}}$), and the steric/geometric properties of the catalyst substituents ($\mathbf{sen}(\boldsymbol{\alpha})$) play the most important role in the success of the reaction. Additionally, the presence of $\boldsymbol{E}_{\mathbf{AB}}$ suggests a specific molecular recognition, in which the catalyst typically prefers to react with substrates in conformation **A**.

In conclusion, the mechanism of the CAPT-catalyzed oxidative amination of tetrahydroisoquinolines has been revisited. The mathematical model previously developed by our groups provided improvement of the reaction performance by extrapolation of a better-performing catalyst (**1a**). In this previous study, mechanistic elucidation with respect to the role of the triazole group was possible, yet the complex equation (13 terms with 9 parameters) did not allow a clear understanding of the mode of coordination between the catalyst and the reactive intermediate **3**.[2b] The strategy presented herein applies computed interaction energies and corresponding distances to access more detailed mechanistic information. The use of the uncatalyzed reaction TSs has been introduced as a new general strategy to compute parameters for intramolecular processes. Similarly, conformational relative energies have also been introduced to describe the conformational freedom of substrate **2**. This new set of parameters allowed us to obtain a significantly simplified multidimensional model, which clearly suggests the role of the catalyst triazole ring in the TS. In particular, it was hypothesized to be involved in the coordination of the substrate through electrostatic interaction with the alkyl portion next to the charged N atom of intermediate **3**. Additionally, the conformational freedom of the substrate was proposed to be important for optimal molecular recognition by the catalyst. We foresee the new parameters and parameterization strategy reported herein to form a useful tool in MCA, as they allow access to detailed mechanistic information even for complex catalytic systems.

Acknowledgements

We thank the NIH (1 R01 GM121383) for support of this research. M.O. thanks the Ermenegildo Zegna Group for a postdoctoral fellowship. Computations were conducted at the Center for High Performance Computing (CHPC) of the University of Utah. We thank Dr. M. J. Hilton for helpful discussions.

Conflict of interest

The authors declare no conflict of interest.

Keywords: asymmetric catalysis · chiral-anion phase-transfer catalysis · free-energy relationships · molecular parameterization · multidimensional correlation analysis

How to cite: *Angew. Chem. Int. Ed.* **2017**, *56*, 14080–14084
Angew. Chem. **2017**, *129*, 14268–14272

[1] a) M. S. Sigman, K. C. Harper, E. N. Bess, A. Milo, *Acc. Chem. Res.* **2016**, *49*, 1292; b) C. Yang, E.-G. Zhang, X. Li, J.-P. Cheng, *Angew. Chem. Int. Ed.* **2016**, *55*, 6506; *Angew. Chem.* **2016**, *128*, 6616; c) T. Piou, F. Romanov-Michailidis, M. Romanova-Michaelides, K. E. Jackson, N. Semakul, T. D. Taggart, B. S. Newell, C. D. Rithner, R. S. Paton, T. Rovis, *J. Am. Chem. Soc.* **2017**, *139*, 1296; d) C. Yang, J. Wang, Y. Liu, X. Ni, X. Li, J.-P. Cheng, *Chem. Eur. J.* **2017**, *23*, 5488; e) H. Huang, H. Zong, G. Bian, H. Yue, L. Song, *J. Org. Chem.* **2014**, *79*, 9455.

[2] a) K. C. Harper, M. S. Sigman, *Science* **2011**, *333*, 1875; b) A. Milo, A. J. Neel, F. D. Toste, M. S. Sigman, *Science* **2015**, *347*, 737; c) C. Zhang, C. B. Santiago, J. M. Crawford, M. S. Sigman, *J. Am. Chem. Soc.* **2015**, *137*, 15668.

[3] a) Z.-M. Chen, M. J. Hilton, M. S. Sigman, *J. Am. Chem. Soc.* **2016**, *138*, 11461; b) Z. L. Niemeyer, A. Milo, D. P. Hickey, M. S. Sigman, *Nat. Chem.* **2016**, *8*, 610; c) J.-Y. Guo, Y. Minko, C. B. Santiago, M. S. Sigman, *ACS Catal.* **2017**, *7*, 4144; d) M. Orlandi, J. A. S. Coelho, M. J. Hilton, F. D. Toste, M. S. Sigman, *J. Am. Chem. Soc.* **2017**, *139*, 6803.

[4] L. P. Hammett, *J. Am. Chem. Soc.* **1937**, *59*, 96.

[5] C. A. Tolman, *Chem. Rev.* **1977**, *77*, 313.

[6] M. Charton, *J. Am. Chem. Soc.* **1975**, *97*, 1552.

[7] R. W. Taft, *J. Am. Chem. Soc.* **1953**, *75*, 4538.

[8] a) H. Clavier, S. P. Nolan, *Chem. Commun.* **2010**, *46*, 841; b) T. Dröge, F. Glorius, *Angew. Chem. Int. Ed.* **2010**, *49*, 6940; *Angew.*

Chem. **2010**, *122*, 7094; c) K. Wu, A. G. Doyle, *Nat. Chem.* **2017**, DOI: https://doi.org/10.1038/nchem.2741.

[9] a) K. C. Harper, E. N. Bess, M. S. Sigman, *Nat. Chem.* **2012**, *4*, 366; b) A. Milo, E. N. Bess, M. S. Sigman, *Nature* **2014**, *507*, 210; c) V. Mougel, C. B. Santiago, P. A. Zhizhko, E. N. Bess, J. Varga, G. Frater, M. S. Sigman, C. Copéret, *J. Am. Chem. Soc.* **2015**, *137*, 6699; d) C. B. Santiago, A. Milo, M. S. Sigman, *J. Am. Chem. Soc.* **2016**, *138*, 13424.

[10] a) V. Rauniyar, A. D. Lackner, G. L. Hamilton, F. D. Toste, *Science* **2011**, *334*, 1681; b) R. J. Phipps, K. Hiramatsu, F. D. Toste, *J. Am. Chem. Soc.* **2012**, *134*, 8376; c) A. D. Lackner, A. V. Samant, F. D. Toste, *J. Am. Chem. Soc.* **2013**, *135*, 14090; d) R. J. Phipps, F. D. Toste, *J. Am. Chem. Soc.* **2013**, *135*, 1268; e) H. M. Nelson, S. H. Reisberg, H. P. Shunatona, J. S. Patel, F. D. Toste, *Angew. Chem. Int. Ed.* **2014**, *53*, 5600; *Angew. Chem.* **2014**, *126*, 5706; f) X. Yang, R. J. Phipps, F. D. Toste, *J. Am. Chem. Soc.* **2014**, *136*, 5225; g) W. Zi, Y.-M. Wang, F. D. Toste, *J. Am. Chem. Soc.* **2014**, *136*, 12864; h) H. M. Nelson, B. D. Williams, J. Miró, F. D. Toste, *J. Am. Chem. Soc.* **2015**, *137*, 3213; i) E. Yamamoto, M. J. Hilton, M. Orlandi, V. Saini, F. D. Toste, M. S. Sigman, *J. Am. Chem. Soc.* **2016**, *138*, 15877; j) Z. Yang, Y. He, F. D. Toste, *J. Am. Chem. Soc.* **2016**, *138*, 9775.

[11] A. J. Neel, J. P. Hehn, P. F. Tripet, F. D. Toste, *J. Am. Chem. Soc.* **2013**, *135*, 14044.

[12] S. Grimme, *J. Comput. Chem.* **2006**, *27*, 1787.

[13] a) R. Valero, J. R. B. Gomes, D. G. Truhlar, F. Illas, *J. Chem. Phys.* **2008**, *129*, 124710; b) Y. Zhao, D. G. Truhlar, *Theor. Chem. Acc.* **2008**, *120*, 215.

[14] a) L. E. Zimmer, C. Sparr, R. Gilmour, *Angew. Chem. Int. Ed.* **2011**, *50*, 11860; *Angew. Chem.* **2011**, *123*, 12062; b) T. J. Seguin, S. E. Wheeler, *ACS Catal.* **2016**, *6*, 7222; c) T. J. Seguin, S. E. Wheeler, *Angew. Chem. Int. Ed.* **2016**, *55*, 15889; *Angew. Chem.* **2016**, *128*, 16121; d) T. J. Seguin, S. E. Wheeler, *ACS Catal.* **2016**, *6*, 2681; e) S. E. Wheeler, T. J. Seguin, Y. Guan, A. C. Doney, *Acc. Chem. Res.* **2016**, *49*, 1061; f) F. Duarte, R. S. Paton, *J. Am. Chem. Soc.* **2017**, *139*, 8886.

Manuscript received: July 26, 2017
Accepted manuscript online: September 13, 2017
Version of record online: October 4, 2017

